Geometry of power flows and convex-relaxed power flows in distribution networks with high penetration of renewables

Huang, Shaojun; Wu, Qiuwei; Zhao, Haoran; Liu, Zhaoxi

Published in:
Energy Procedia

Link to article, DOI:
10.1016/j.egypro.2016.10.134

Publication date:
2016

Document Version
Publisher's PDF, also known as Version of record

Available online at www.sciencedirect.com

ScienceDirect

Energy Procedia 100 (2016) 1 – 7

Energy Procedia

3rd International Conference on Power and Energy Systems Engineering, CPESE 2016, 8-12 September 2016, Kitakyushu, Japan

Geometry of power flows and convex-relaxed power flows in distribution networks with high penetration of renewables

Shaojun Huang[a]*, Qiuwei Wu[a], Haoran Zhao[a], Zhaoxi Liu[a]

[a]*Centre for Electric Power and Engineering, Technical University of Denmark, Elektrovej, Building 325, 2800 Lyngby, Denmark*

Abstract

Renewable energies are increasingly integrated in electric distribution networks and will cause severe overvoltage issues. Smart grid technologies make it possible to use coordinated control to mitigate the overvoltage issues and the optimal power flow (OPF) method is proven to be efficient in the applications such as curtailment management and reactive power control. Nonconvex nature of the OPF makes it difficult to solve and convex relaxation is a promising method to solve the OPF very efficiently. This paper investigates the geometry of the power flows and the convex-relaxed power flows when high penetration level of renewables is present in the distribution networks. The geometry study helps understand the fundamental nature of the OPF and its convex-relaxed problem, such as the second-order cone programming (SOCP) problem. A case study based on a three-node system is used to illustrate the geometry profile of the feasible sub-injection (injection of nodes excluding the root/substation node) region.

Peer-review under responsibility of the organizing committee of CPESE 2016

Keywords: Power flow; Convex relaxation; Distribution network; Distributed energy resources

1. Introduction

The integration of more and more renewable energies, such as wind power (WP) and solar power (SP), into distribution networks becomes a big challenge to distribution system operations. The impacts on the distribution networks due to high penetration of these distributed generators (DG) include overvoltage and overloading issues. Extensive research has been carried out to deal with these issues. In [1], a local voltage control method based on voltage sensitivity to reactive power injection was proposed. The development of information communication technologies for smart grid enables the voltage control methods based on centralized coordination. In [2], two coordinated control methods, i.e. the rule based method and the optimal power flow (OPF) based method, were proposed. The OPF based method has better economic efficiency because it tries to minimize the active power curtailment of the DGs and the power losses of the network. The OPF problems are difficult to solve to the global

* Corresponding author. Tel.: +45 45 25 34 95.
E-mail address: shuang@elektro.dtu.dk.

Peer-review under responsibility of the organizing committee of CPESE 2016
doi:10.1016/j.egypro.2016.10.134

optimum due to the non-convexity. In order to solve the OPF problem for optimal curtailment of DGs, linear approximations were made based on sensitivity analysis in [3].

More accurate methods are needed for solving the OPF problems formed for applications of energy management in distribution networks, such as the congestion management due to DGs and/or flexible demands including electric vehicles (EV) and heat pumps (HP). The convex relaxation method for solving the AC OPF was first presented in [4] as a second-order cone programming (SOCP) for radial networks and in [5] as a semidefinite programming (SDP) for meshed networks. In [6], a sufficient condition which has requirements on the upper limit of the active and reactive power injections was proposed for the convex relaxation of the OPF problem to be exact. Another sufficient condition proposed in [7] ensures the exactness of the convex relaxation and the convexity of the feasible sub-injection (the injection of the nodes excluding the root node of the network) region when the active reverse power flow is not heavy. However, neither of these sufficient conditions is valid for the applications discussed in [1]–[3] where heavy active reverse power flows are present.

In this paper, the OPF for applications with heavy active reverse power flows will be investigated. The main contributions of this paper include: (a) Visualize the geometry boundary of the feasible sub-injection of the OPF through a case study based on a three-node system; (b) Visualize the geometry boundary of the feasible sub-injection region of the convex-relaxed OPF; (c) Show that the sub-injection region is nonconvex when the reverse power flow is heavy.

The paper is organized as follows. Section 2 introduces the formulation of the OPF problem and its convex relaxation. Section 3 presents the methodology for visualizing the geometry boundary of the sub-injection for both the original OPF and the convex-relaxed one. A case study based on a three-node system is described in Section 4, followed by conclusions.

2. Optimal power flow and concept of sub-injection region

2.1. Optimal power flow based on branch flow model

OPF problems can be employed for applications such as minimizing the curtailment of the renewables or equivalently maximizing the sub-injection. An OPF based on the branch flow mode [8] is written as (1)-(7). Notice that the distribution network operates in tree configuration. The substation is deemed as the root node, denoted as 0, of the tree. An edge, denoted as (i, j) or $i \to j$, of the tree is a segment of the feeder and the direction is pointing to the root, implying that i is a child node of j.

OPF:

$$\max_{s,S,\mathbf{v},\mathbf{i},s_0} \sum_{i\in\mathcal{N}^+} c_i \operatorname{Re}(s_i), \tag{1}$$

s.t.

$$S_{ij} = s_i + \sum_{h:h\to i} (S_{hi} - z_{hi}\mathbf{i}_{hi}), \forall (i,j) \in \mathcal{E}, \tag{2}$$

$$0 = s_0 + \sum_{h:h\to 0} (S_{h0} - z_{h0}\mathbf{i}_{h0}), \tag{3}$$

$$\mathbf{v}_i - \mathbf{v}_j = 2\operatorname{Re}(\overline{z}_{ij} S_{ij}) - \left|z_{ij}\right|^2 \mathbf{i}_{ij}, \forall (i,j) \in \mathcal{E}, \tag{4}$$

$$\mathbf{i}_{ij} = \frac{\left|S_{ij}\right|^2}{\mathbf{v}_i}, \forall (i,j) \in \mathcal{E}, \tag{5}$$

$$\underline{s}_i \le s_i \le \overline{s}_i, \forall i \in \mathcal{N}^+, \tag{6}$$

$$\underline{\mathbf{v}}_i \le \mathbf{v}_i \le \overline{\mathbf{v}}_i, \forall i \in \mathcal{N}^+, \tag{7}$$

where c_i is the coefficient, s_i is the sub-injection at node i, including the net active and reactive power injected at the node, S is the branch flow, $\mathbf{v}$ is the square of the voltage magnitude, $\mathbf{i}$ is the square of the current magnitude, z is the impedance, s_0 is the injection of the root node, i.e. the injection from the bulk grid, $\mathcal{E}$ is the set of edges, $\mathcal{N}^+$ is the set of nodes excluding the root node.

The objective function (1) is to maximize the sub-injection (let c_i =1), i.e. minimize the curtailment of renewables. Constraints (2)-(5) are the load flow equations. Constraint (6) gives the limits of the net sub-injections. Constraint (7) presents the voltage limits.

Its convex relaxation as an SOCP is shown below [8]. The nonlinear equation (5) is modified to be a conic inequality (8), which makes the OPF an SOCP.

SOCP:

$$\text{(1)}$$

s.t.

$$\text{(2)-(4), (6)-(7), and}$$

$$\mathbf{i}_{ij} \geq \frac{|S_{ij}|^2}{\mathbf{v}_i}, \forall (i,j) \in \mathcal{E}. \qquad \text{(8)}$$

2.2. Concept of sub-injection

The concept of the feasible sub-injection region is introduced in [7]. As shown in [9], [10], the feasible set $\mathcal{P}$ defined below, known as the feasible injection region, is normally non-convex. However, if the focus is put on the feasible injection region of p (active power injection of plus nodes $\mathcal{N}^+$, $p = \mathrm{Re}(s)$), the feasible set can be proven to be convex under the condition proposed in [7]. This partial injection region can be named as the feasible sub-injection region, $\mathcal{P}^+$. Set $\mathcal{P}^+$ is an orthogonal projection of $\mathcal{P}$ to the subspace of vector p.

$$\mathcal{P} = \{ p_0, p : \text{(2)-(7)} \},$$

$$\mathcal{P}^+ = \{ p : \text{(2)-(7)} \},$$

where $p_0 = \mathrm{Re}(s_0)$ and $p = \mathrm{Re}(s)$.

3. Methodology of visualizing the feasible sub-injection region

For linear objective functions, such as (1), in the OPF problems, it is important to know the boundary of the feasible set because the optimal solutions are on the boundary. Numerical methods are employed in this paper to investigate the boundary. The focus will be given to the boundary of the sub-injection, since the objective function is only depending on the sub-injection.

In order to determine the boundary of the sub-injection, samples are taken from the boxing area defined by (6). The net injection s is considered to be positive, since this paper focuses on the heavy reverse power flow situation. The sample sub-injection s is employed to calculate the voltage profile through power flow analysis tools, such as Newton-Raphson method. Node 0 is chosen to be the slack node and its voltage is 1 p.u. After determining the voltage profile, the voltage at the end of the feeder is compared with the upper limit defined by(7). If the voltage fulfils (7), the sample sub-injection is in the feasible region; otherwise, it is outside of the feasible region. The boundary is determined after processing enough samples.

For the SOCP, the boundary is determined through changing the coefficient $c_i > 0$ and solving the corresponding SOCP, since the optimal solution must be located on the boundary. Due to the convex nature of the boundary for the SCOP, it is possible to determine the boundary by taking large number of samples of the coefficient c_i and solve the corresponding SOCPs.

4. Case study

The case study is carried out with a three-node system, which can ease the view of the geometry boundary of the sub-injection. Although it is a special case of the general distribution networks, the results of the three-node system can illustrate the geometry of the power flows of general distribution networks.

The three-node system is shown in Fig. 1. Node 0 is the root node, or the substation, and s_0 is the injection from the bulk grid. The subscripts of z_{ij}, $\mathbf{i}_{ij}$, S_{ij} are shorted as z_i, $\mathbf{i}_i$, S_i without causing confusion since the parent node is always unique for a given child node in a tree graph. The positive direction of the current and power flow is

pointing towards the root node. The impedance is chosen to be $z=[z_1,z_2]$=[1.76+0.52j, 4+2.4j] ohm. The per-unit (p.u.) system is employed in the calculation. The base voltage is 11 kV and the base power is 11 MVA. Voltage of node 0 is 1 p.u. and the upper limit of the voltage is 1.05 p.u.

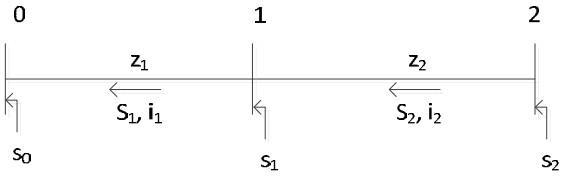

Fig. 1 A three-node system. Node 0 is the root node, or the substation, and S_0 is the injection from the bulk grid.

4.1. Case study results

Matlab is employed to perform the power flow analysis to determine the geometry boundary of the sub-injection for the original OPF. Matlab/CVX is employed to solve the SOCP and determine the boundary of the sub-injection of the convex-relaxed power flow.

4.1.1. Case One

Case One is the base case. The reactive power is chosen to be $q=[q_1,q_2]$=[0.1j, 0.1j]. The active power p_1 is varying between zero and the upper limit with small steps. The corresponding active power p_2 is determined such that the voltage at node 2, which is the critical node for overvoltage issues, is the upper limit 1.05 p.u. The boundary can be drawn through many such pairs $[p_1,p_2]$, shown as the solid line in Fig. 2. The feasible sub-injection is formed by joining the solid line and the two axes (left axis of p_1 and the bottom axis of p_2).

By connecting the two vertexes with a straight line, shown as the dashed line in Fig. 2, it can be seen that the feasible sub-injection region is concave in this case. The dashed line, combining the axis of p_1 and p_2, forms the convex hull of the sub-injection region. In order to determine the convex-relaxed boundary, the method described in Section 3 is employed. It is worthwhile to mention that the current magnitude is limited between zero and the maximum current magnitude in the process of determining the boundary for the original OPF. Otherwise, the convex-relaxed boundary would be too large and become less useful. The final convex-relaxed boundary is shown as the dotted line in Fig. 2. It can be seen that the convex-relaxed boundary of the sub-injection for the SOCP is not the same as the convex hull.

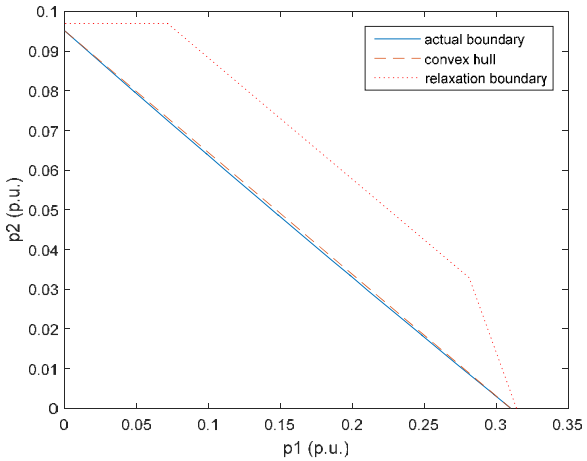

Fig. 2. Results of Case One.

4.1.2. Case Two

In Case Two, the reactive power injection is the same as the base case, but the resistance is modified to be half of the base case such that the R/X ratio is decreased. This means the new impedance $z^{(2)} = 0.5r + \mathrm{j}x$, where $z = r + \mathrm{j}x$ is the impedance of the base case.

The results are shown in Fig. 3. It can be seen that the feasible sub-injection region becomes larger because of the reduced resistance. On the other hand, the sub-injection becomes more concave compared to the base case.

4.1.3. Case Three

In Case Three, the reactive power injection is the same as the base case. The impedance is modified to be $z^{(3)} = 0.5r + \mathrm{j}2x$, such that the R/X ratio is further decreased. The results are plotted in Fig. 4. It can be seen that the size of the feasible sub-injection region doesn't change much compared to Case Two, because the active power injection isn't sensitive to the change of the reactance as long as the R/X ratio is not too small, such as the R/X ratio for transmission lines. It can also be seen that the feasible sub-injection region becomes even more concave.

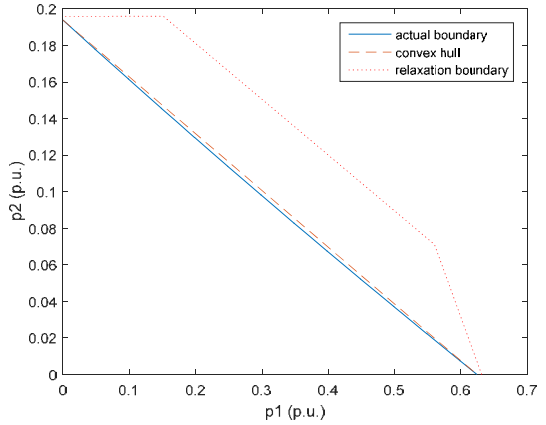

Fig. 3 Results of Case Two.

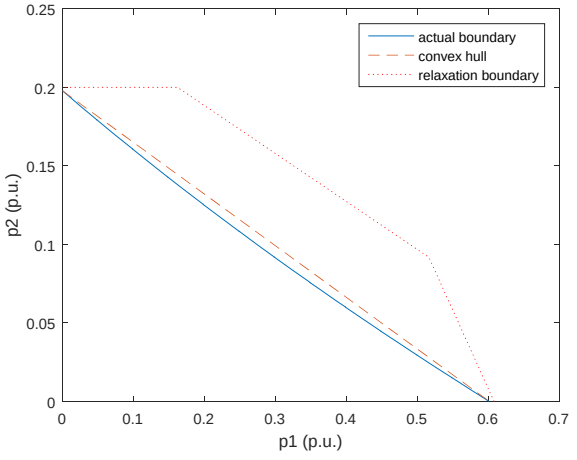

Fig. 4 Results of Case Three.

4.1.4. Case Four

In Case Four, the impedance is the same as Case Two, i.e. $z^{(4)} = 0.5r + \mathrm{j}x$. But the reactive power injection becomes negative, i.e. $q^{(4)} = -q$, implying that the customers at node 1 and 2 are consuming reactive power. The boundaries are calculated and shown in Fig. 5. It can be seen that the maximum allowed p_1 and p_2, inside of the feasible sub-injection region, is improved compared to Case Two. This is because the reactive consumption helps

reduce the node voltages and therefore ease the overvoltage issue caused by the renewables. On the other hand, the concaveness of the sub-injection region is similar to Case Two.

4.1.5. Case Five

In Case Five, the impedance is the same as Case Three, i.e. $z^{(5)} = 0.5r + \mathrm{j}2x$. The reactive power is the same as Case Four, i.e. $q^{(5)} = -q$. The results are shown in Fig. 6. Similar conclusions can be made through the comparison of Case Five and Case Three, and the comparison of Case Four and Case Two. The size of the feasible sub-injection region is improved; however, the concaveness is similar, compared to Case Three.

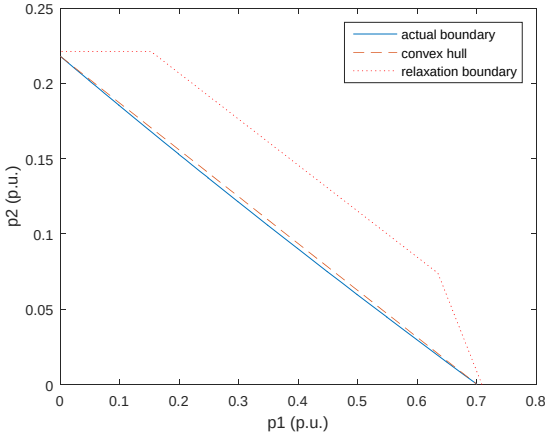

Fig. 5. Results of Case Four.

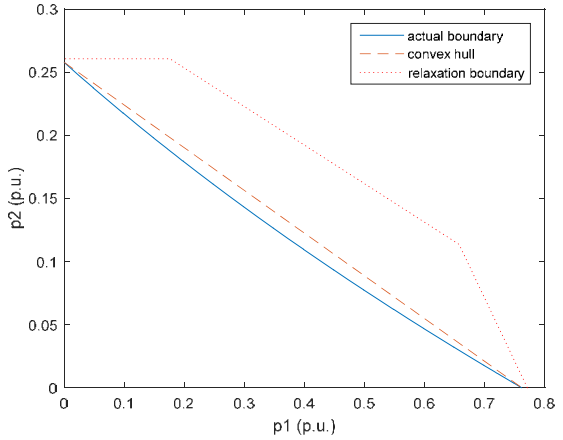

Fig. 6. Results of Case Five.

4.2. Discussion

Through the above case studies, some general statements can be made regarding the geometry of the power flows. First of all, the feasible sub-injection region is not convex when there are heavy reverse power flows. Second of all, when R/X ratio is high, the boundary of the sub-injection is very close to its convex hull. For the special case of the three-node system, the convex hull consists of linear combinations of extreme sub-injections. The extreme sub-injections are achieved by letting all but one active power injection be zero. At last, the convex-relaxed boundary is always larger than the convex hull. Therefore, caution must be made when employing the SOCP to solve the original OPF.

5. Conclusion

This paper has investigated the geometry of the power flows and the convex-relaxed power flows of distribution networks through numerical methods. It is observed from the case studies that the sub-injection of the original OPF is not convex. The boundary of the sub-injection is close to its convex hull but has a big gap to the convex-relaxed boundary. In the future, improvements will be made before the SOCP method can be employed to solve the OPF problems when heavy reverse power flows are present in the distribution networks.

References

[1] E. Demirok, P. C. González, K. H. B. Frederiksen, D. Sera, P. Rodriguez, and R. Teodorescu,“Local reactive power control methods for overvoltage prevention of distributed solar inverters in low-voltage grids,” *IEEE J. Photovoltaics*, vol.1, no.2, pp. 174–182, 2011.
[2] A. Kulmala, S. Repo, and P. Jarventausta,“Coordinated voltage control in distribution networks including several distributed energy resources,” *IEEE Trans. Smart Grid*, vol.5, no.4, pp. 2010–2020, Jul. 2014.
[3] Q. Zhou and J. W. Bialek,“Generation curtailment to manage voltage constraints in distribution networks,” *IET Gener. Transm. Distrib.*, vol.1, no.3, pp. 492 – 498, May 2007.
[4] R. A. Jabr,“Radial distribution load flow using conic programming,” *IEEE Trans. Power Syst.*, vol.21, no.3, pp. 1458–1459, Aug. 2006.
[5] X. Bai, H. Wei, K. Fujisawa, and Y. Wang,“Semidefinite programming for optimal power flow problems,” *Int. J. Electr. Power Energy Syst.*, vol.30, no.6–7, pp. 383–392, Jul. 2008.
[6] L. Gan, N. Li, U. Topcu, and S. H. Low,“Exact convex relaxation of optimal power flow in radial networks,” *IEEE Trans. Automat. Contr.*, vol.60, no.1, pp. 72–87, Jan. 2015.
[7] S. Huang, Q. Wu, J. Wang, and H. Zhao,“A sufficient condition on convex relaxation of AC optimal power flow in distribution networks,” *IEEE Trans. Power Syst.*, (Accepted).
[8] M. Farivar and S. H. Low,“Branch flow model: relaxations and convexification—Part I,” *IEEE Trans. Power Syst.*, vol.28, no.3, pp. 2554–2564, Aug. 2013.
[9] B. Zhang and D. Tse,“Geometry of injection regions of power networks,” *IEEE Trans. Power Syst.*, vol.28, no.2, pp. 788–797, May 2013.
[10]B. Zhang and D. Tse,“Geometry of feasible injection region of power networks,” in *Proc. 2011 49th Annual Allerton Conference on Communication, Control, and Computing (Allerton)*, pp. 1508–1515.